

gains. However, these materials do not allow reasonable working time at higher temperatures. The freeze-thaw performance of the modified portland cement and the gypsum-modified portland cement was significantly better than for the magnesium phosphate and the magnesium polyphosphate.

#### ACKNOWLEDGMENTS

The authors wish to acknowledge the support provided by the Texas Department of Highways and Public Transportation and the Federal Highway Administration, U.S. Department of Transportation, for the funding of this research.

#### REFERENCES

1. P.E. Irick. Rapid-Setting Materials for Patching of Concrete. In NCHRP Report 45. TRB, National Research Council, Washington, D.C., 1977, 13 pp.
2. G.P. Beer, D.W. Fowler, A.H. Meyer, and D.R. Paul. Results of a Survey on the Use of Rapid-Setting Repair Materials. Research Report 311-1. Center for Transportation Research, The University of Texas, Austin, Dec. 1982.

The opinions expressed are those of the authors and not necessarily of the sponsoring agencies.

## Shear Transfer in Two-Layer Composite Systems

EDWARD G. NAWY

#### ABSTRACT

Experiments were conducted to evaluate the shear transfer capacity of two-layered systems using polymer-modified concrete as the top layer. The experimental program was designed to verify the general theory of shear transfer mechanism for concrete and to evaluate the necessary constants of the theoretical expressions. The general theory presented covers structural members with (a) no shear reinforcement, (b) moderate shear reinforcement, and (c) high shear reinforcement. Four groups of specimens were tested. Group A specimens were used to investigate the relation between intrinsic bond shear transfer capacity and the strength of the composite materials. Group B specimens contained various amounts cast monolithically using ordinary concrete to serve as control specimens. Group C contained control specimens made up of totally cast-in-place concrete with no cold joints. Group D contained control specimens made up of cast-in-place concrete over precast concrete.

The problem of shear transfer in concrete structures arises when shearing loads must be transmitted across a definite and often weak plane. Typical situations are encountered in corbels, nonmonolithic joints in concrete, and composite elements where concrete is cast in place over a precast member.

Since the early 1950s, several researchers have studied this problem. It is generally recognized that the shear transfer capacity in concrete elements can be attributed to any of the following: friction at the shear plane, interlocking action of the aggregates, dowel action of any reinforcement,

and bond forces (apparent cohesion) at the shear plane. However, there continues to be a great deal of debate regarding the relative importance of the various parameters.

Of the many expressions for shear transfer capacity (1-12), the simplest and most widely used has been that based on the shear friction hypothesis of Birkeland and Birkeland (1). This expression with minor modification (9) has been incorporated in the American Concrete Institute (ACI) code. Although the expression is useful in estimating shear transfer capacities, its very formulation ignores "apparent cohesion" (bond) and dowel action resistance.

This paper is a condensation of "Shear Transfer in Concrete and Polymer Modified Concrete Members Subjected to Shearing Loads" (2), which deals with the shear capacity of the normal concrete-polymer modified concrete interface. A general theory on the shear transfer mechanism is also presented correlating with the tests (13,14). The discussion covers any two-layered system.

#### A THEORY OF SHEAR TRANSFER MECHANISM FOR CONCRETE

It is hypothesized that the total shear transfer capacity in a concrete element is made up of: intrinsic bond shear resistance,  $\Delta V_b$ ; shear friction resistance,  $\Delta V_f$ ; aggregate interlock resistance,  $\Delta V_i$ ; and dowel resistance,  $\Delta V_d$ .

Consider an element subjected to a shearing load (Figure 1). Initially, all shear resistance is provided by intrinsic bond. After cracking has started and some slip has occurred, resistance is developed through friction, aggregate interlock, and dowel action. Shear transfer through friction is due purely to the surface shear resistance to slip. Aggregate interlock is due to the interlocking action of the aggregates at the failure plane. Dowel action shear resistance is a result of the steel reinforcement as shown in part b of Figure 1.

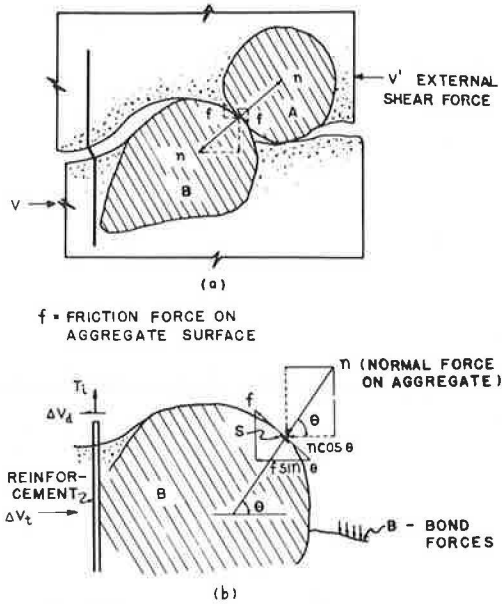


FIGURE 1 Idealized shear resisting forces [shear resistance through friction ( $f \sin \theta$ ), aggregate interlock ( $n \cos \theta$ ), and dowel action  $V_d$ ].

Summing up the resistances in the horizontal direction gives

$$V_t = \Delta V_b + \Delta V_f + \Delta V_i + \Delta V_d \quad (1)$$

and the nominal shear transfer capacity becomes

$$v_t = \left[ \int_A \Delta V_t \right] / A \quad (2)$$

where  $A$  is area of the shear plane. (Note: a list of notations used in the equations appears at the end of this paper.)

By idealizing concrete mass as brittle material containing micro-cracks, it has been shown that bond shear strength is an intrinsic property of any given concrete (13). The resistance due to bond can be represented by  $v_b = B d A$ , where  $B$  is strength per unit bond area.

If  $n'$  is the total number of bars, and  $T_f$  is the load transferrable by dowel action per bar, the expression for the total dowel force from Dulacska (4) modified such that the shear reinforcement is taken normal to the fracture plane yields a total dowel force.

$$n' T_f = [4 A_s' / \pi] \left\{ [1 - (f_s / f_y)^2] 1.51 f_c' / f_y \right\}^{1/2} \quad (3)$$

The shear stress over the cross-sectional area  $bw$  of the failure plane is  $v_d = (n' T_f) / bw$ . If  $\bar{\rho} = n' A_s' / bw$  = steel ratio for shear transfer reinforcement, then:

$$v_d = [4 \bar{\rho} f_y / \pi] \left\{ [1 - (f_s / f_y)^2] 1.51 f_c' / f_y \right\}^{1/2} \quad (4)$$

where  $v_d$  represents dowel action shear resistance. This expression incorporates the condition that as the tension force in the shear reinforcing steel approaches the yield point,  $v_d$  tends to become zero.

For friction and aggregate interlock, the contribution of the surface frictional force to transfer strength (Figure 1) is expressed as

$$v_f = f \sin \theta \quad (5)$$

where  $f$  is frictional force on the surface. The contribution due to aggregate interlock is

$$v_i = n \cos \theta \quad (6)$$

where  $n$  is normal force per unit area. If  $T_i$  = tension force in the steel per unit area =  $\bar{\rho} f_s$ , summing forces in the direction  $n$  gives

$$v_n = (\bar{\rho} f_s + B d A) \sin \theta - v_d \cos \theta$$

Frictional force  $f = \mu n$  where  $\mu$  is the coefficient of friction between the aggregate and the cement mortar surrounding it.

Recollecting terms and integrating these forces over the surface area of the aggregates and dividing by the cross-sectional area of the failure plane, the resistance  $v_f$  due to friction and  $v_i$  due to aggregate interlock can be defined as follows:

$$v_f = \mu [(\bar{\rho} f_s + B k_1) \pi / 4 - 1/2 v_d] k_2 + \mu (\bar{\rho} f_s + B k_1) k_3 \quad (7)$$

$$v_i = [\bar{\rho} f_s + B k_1] \pi - 1/2 v_d k_2 \quad (8)$$

where

- $k_1$  = ratio of bond area to total shear area,
- $k_2$  = ratio of projected area of aggregates to total shear area,
- $k_3 = 1 - k_1 - k_2$ , and
- $B$  = bond shear strength for unit area.

The detailed derivation of Equations 7 and 8 can be found in Ukadike (13, pp. 145-149).

Adding the various components of resistance and rearranging terms gives

$$v_t = B k_1 + (4 \bar{\rho} f_y / \pi) \left\{ [1 - (f_s / f_y)^2] 1.51 f_c' / f_y \right\}^{1/2} \left\{ 1 - k [1 + (\mu / 2)] \right\} + (\bar{\rho} f_s + B k_1) \left\{ \mu k_3 + k_2 \pi (\mu / 4 + 1) \right\} \quad (9)$$

#### Members with No Shear Reinforcement

When no shear reinforcement is provided (i.e.,  $\bar{\rho} = 0$ ) Equation 9 reduces to:

$$v_t = B k_1 + B k_1 [\mu k_3 + k_2 \pi (\mu / 4 + 1)] = C_o \text{ (a constant)} \quad (10)$$

This may be written as

$$C_o = B k_1 (1 + \mu) = \text{"apparent cohesion"} \quad (11)$$

where  $\mu' = [\mu k_3 + k_2 \pi (\mu / 4 + 1)]$  = apparent coefficient of friction.

The term  $B k_1$  is the value of shear transfer capacity that would be developed if there were no coarse aggregates at the shear plane (i.e., in mortars). The other term,  $B k_1 \mu'$ , is due to aggregate interlock and friction forces made possible by the intrinsic bond force, which creates a compression on the failure surfaces. The factors  $\pi/4$ ,  $1/\pi$ , and  $1/2$  reflect the shape of the aggregates (assumed spherical) in the concrete mix. The constants  $k_1$  and  $k_2$  depend on the concrete strength and aggregate ratio, respectively, as the definitions of  $k_1$  and  $k_2$  imply.

#### Members with Moderate Shear Reinforcements

If a moderate amount of shear reinforcement is provided (Figures 2 and 3), shear failure will be pre-

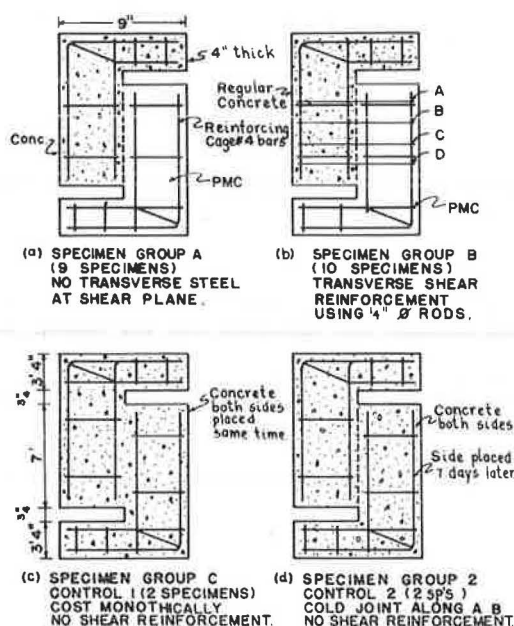


FIGURE 2 Test specimen groups.

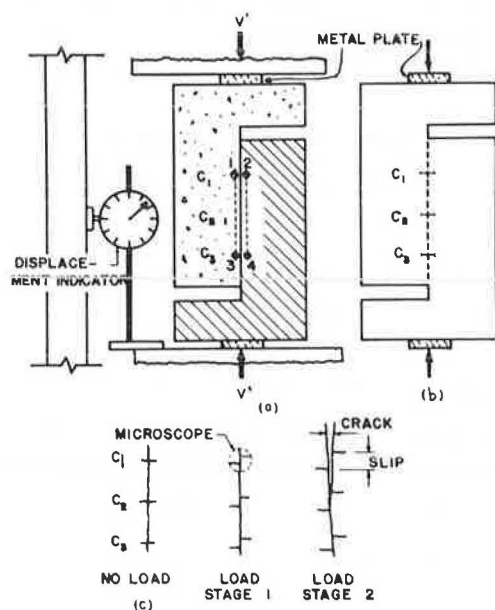


FIGURE 3 Instrumentation of L-prism specimens.

ceded by the yielding of the reinforcement, that is,  $f_s = f_y$ .

Therefore,

$$v_t = (Bk_1) + (\bar{\rho}f_y + Bk_1) [\mu k_3 + k_2 \pi(\mu/4 + 1)] \quad (12)$$

Rearranging the expression and grouping constant terms yields

$$v_t = \bar{\rho}f_y \times \mu' + C' \quad (13)$$

$$= I \times \mu' + C' \quad (14)$$

where  $C' = (Bk_1)(1 + \mu')$  and  $I = \bar{\rho}f_y$  (defined as shear reinforcing strength).

Experimental investigations show that the addition of shear reinforcement results in a rapid increase of

$v_t$ . This is because an increase in the value of  $I$  not only provides compression at the shear surface, but also inhibits cracking, with the new higher value of the apparent cohesion  $C'$  at  $\bar{\rho} > 0$  as compared to apparent cohesion  $C$  at  $\bar{\rho} = 0$ .

Equation 13 is similar to that proposed by Hermansen and Cowan (8). Unlike the shear friction hypothesis, the expression accounts for the shear transfer capacity observed in shear tests where there has been no shear-reinforcing steel.

#### Members Having High Shear Reinforcement

If the shear reinforcing strength ( $\bar{\rho}f_y$ ) is very high, the aggregates on the shear plane may be dislocated or sheared off as load is applied and  $k_1$  and  $k_2$  will equal 0. Shear transfer capacity will then only be due to friction and dowel action of reinforcement.

$$v_t = (4\bar{\rho}f_y/\pi) \left\{ (1.51 f'_c/f_y) [1 - (f_s/f_y)^2] \right\}^{1/2} + \bar{\rho}f_s \mu \quad (15)$$

For a given concrete cracking strength, as  $\bar{\rho}$  increases,  $f_s$  decreases; thus for high values of  $I$ ,  $[1 - (f_s/f_y)^2]$  is almost equal to 1 and  $\bar{\rho}f_s$  becomes a constant.

The expression, therefore, reduces to

$$v_t = GI + Q \quad (16)$$

where  $G = 1.564 (f'_c/f_y)^{1/2}$  and  $Q = \bar{\rho}f_s \mu$ .

If the aggregates are not dislocated, the concrete in the vicinity of the shear plane may fail as a result of the combined stresses (6), namely, direct compressive stress due to transverse steel tension and shear stress due to applied shear load.

#### EXPERIMENTAL INVESTIGATION

Experimental investigation was performed to verify the general form of the derived shear capacity expressions and to determine the values of the constant terms in them. The study dealt with composite elements of precast concrete and cast-in-place PMC. Similar ordinary concrete elements were used as control specimens. The details of the four groups of specimens A, B, C, and D are presented in Figure 2 and Tables 1 and 2.

Group A specimens were used to investigate the relationship between intrinsic bond shear transfer capacity and the strength of the composite materials (PMC and concrete). No transverse steel was used in these specimens. There were three types; the only variable among them was the strength of the PMC.

Group B specimens were for the purpose of verifying the shear transfer capacity expressions developed earlier. For this group, the PMC strength was set at 68.95 MPa (10,000 psi), the same as in specimen Group A, Type II. There were five types in this group, each having a different shear reinforcing strength.

Group C specimens were cast monolithically of ordinary concrete to serve as control specimens to give concrete shear strength. No shear transfer reinforcement was used.

Group D contained control specimens made up of cast-in-place concrete over precast concrete. They were designed to give the apparent cohesion of such elements, for the purpose of comparison with Group A specimens.

TABLE 1 Properties of "L" Prism Shear Tests

Designation		Cylinder Compressive & Tensile Splitting Strengths (PSI)		Shear Reinforcing Strength $I = p_f y$ (PSI)	Specimen Description
Grp	Type No.	Concrete (Side 1)	PMC (Side 2)		
(1)	(2)	(3)	(4)	(5)	(6)
A	1	i	5130 (546)	8120 (774)	-
		ii	5130 (546)	8120 (774)	-
		iii	5130 (546)	8120 (774)	-
	2	i	5130 (546)	10040 (1020)	-
		ii	5130 (546)	10040 (1020)	-
		iii	5130 (546)	10040 (1020)	-
	3	i	5130 (546)	11640 (1222)	-
		ii	5130 (546)	11640 (1222)	-
		iii	5130 (546)	11640 (1222)	-
B	1	i	5540 (562)	9820 (996)	286
		ii	5300 (553)	10300 (1000)	286
	2	i	5540 (562)	9820 (996)	572
		ii	5300 (553)	10300 (1000)	572
	3	i	5540 (562)	9820 (996)	858
		ii	5300 (553)	10300 (1000)	858
	4	i	5540 (562)	9820 (996)	1073
		ii	5300 (553)	10300 (1000)	1073
	5	i	5540 (562)	9820 (996)	1375
		ii	5300 (553)	10300 (1000)	1375
C	i	5130 (546)	5130 (540) concrete	-	Monolithic Concrete Specimen
	ii	5540 (562)	5540 (362)	-	
D	i	5130 (546)	5300 (553) concrete	-	Cold-Jointed Concrete/ Concrete; no reinforcement
	ii	5130 (546)	5300 (553)	-	

### Instrumentation

To observe the behavior of the specimens under loading and determine the onset of failure, the slip and crack widths at the shear plane were measured. Slip was measured using three different methods (Figure 3). Demac discs were installed at positions 1, 2, 3, and 4 on each specimen such that positions 1-4 and 2-3 were about 4 in. apart. During the loading, the distances were measured with a 4-in. mechanical gauge. By subtracting the change in positions 1-4 from that of positions 2-3, the displacement due to other causes can be eliminated and the slip obtained as  $1/2(\Delta_{2-3} - \Delta_{1-4})$  (13). A displacement indicator was also mounted on the loading platform as shown in Figure 3. The readings from the indicator, when corrected for other effects, give a second slip estimate. Three short horizontal lines were drawn at locations  $C_1$ ,  $C_2$ , and  $C_3$  across the shear plane. Slip was determined by measuring the vertical distance between the two displaced parts of each line (part c of Figure 3) by means of a microscope. Crack length was also measured.

### RESULTS OF THE "L" PRISM SHEAR TESTS

#### Observed Behavior of Shear Test Specimens

During the course of the investigation, the following observations were made regarding the behavior of the specimens.

1. In Group A specimens, loading was not accompanied by much slip or cracking until quite close to the ultimate. There was no noticeable vertical strain or lateral bulging in either the PMC or the concrete halves of the specimens. When the cracks finally appeared, they ran parallel to the joint or diagonally into the regular concrete half, at an angle of 40 to 55 degrees. Examination of the failure surface showed that most of the cracking and separation had occurred in the ordinary concrete section near the shear plane.

2. Generally, Group B specimens behaved like those in Group A up to the occurrence of continuous cracks along the shear plane. After this stage, subsequent loading was accompanied by large increases in the crack width and the amount of slippage. Three of the 4 bars in specimens B1i and B1ii broke when the specimens were loaded beyond the yield strength. The failure surface showed considerable smoothing but it was not clear whether the smoothing occurred before or during loading to collapse. The cracks on the specimens having the largest reinforcing strength ( $I = 1,375$  psi) were shorter in length and not as wide as the others.

3. In the case of Group C specimens, the first few load increments caused no visible signs of distress. At a load of about 68.95 MPa (10,000 psi), short diagonal cracks suddenly appeared on the surface, crossing the shear plane at an angle of 40 to 50 degrees, somewhat similar to the cracks that oc-

TABLE 2 Results of the "L" Prism Shear Tests

Test Designation (1)		Shear Reinforcing Strength PSI (2)	Ultimate Shear Transfer Capacity PSI (3)	Failure Mode (4)
A1	i	-	567	Cracking along composite plane; Some slipping and finally separation of the composite sides
	ii	-	547	
	iii	-	571	
A2	i	-	685	
	ii	-	640	
	iii	-	620	
A3	i	-	985	
	ii	-	905	
	iii	-	955	
B1	i	286	855	Slipping along plane; steel yield
	ii	286	877	
B2	i	572	1193	As above
	ii	572	1071	
B3	i	858	1243	Slipping & probable steel yield
	ii	858	1191	
B4	i	1073	1392	As above with cracking
	ii	1073	1304	
B5	i	1375	1428	Extensive cracking; slipping; steel yield unlikely
	ii	1375	1324	
C	i	-	984	Diagonal Cracking; typical Shear Failure
	ii	-	944	
D	i	-	488	Cracking along shear plane; little slip separation of composite sides
	ii	-	500	

Ultimate Shear Transfer Capacity = Force (lbs)/bw  
where b and w are the length and width of the shear surface, respectively

curred in Group A specimens. Failure was preceded by the formation of series of cracks across the concrete struts formed by the previous diagonal cracks. The exposed aggregates were uncracked. Cracking had occurred in the mortar surrounding the aggregates.

4. Control specimens in Group D behaved like those in Group A except that when cracks appeared, they ran mostly along the shear plane. Failure followed the formation of a continuous crack along the shear plane almost immediately. Even in this group, some cast-in-place concrete stuck to the older concrete at the failure surface.

#### Shear, Slip, and Crack Result

The ultimate strength results are given in Table 2. The values represent the average of three or two results. The slips determined by the three different methods described previously are plotted separately. The first, Series I, includes all the composite specimens having no shear reinforcement, that is, Groups A and D. PMC strength was the only variable. Series II includes all the composite specimens in which the PMC strength was constant and the only variable was the shear reinforcing strength.

#### Analysis of Series I Specimen Results

The plots of applied shear stress ( $\tau$ ) versus slip and  $\tau$  versus maximum crack width (Figures 4 and 5) show that:

1. Concrete-PMC composite specimens undergo considerable slip before failure. In contrast, the concrete control specimens failed suddenly.

2. Ultimate shear transfer capacity increases with increasing PMC strength.

3. The slopes of the curves increase with increasing PMC strength.

4. The slip at yield appears to be almost constant at 0.5 mm (0.02 in.).

5. The shear transfer capacity of the specimens having a PMC strength of 82.74 MPa (12,000 psi) is about the same as that of the monolithically cast ordinary concrete specimens.

The polymer at the composite interface creates a bond between the precast concrete and the cast-in-place PMC. It has been shown that this bond is in the form of polymer fibers bridging the micro-cracks in the specimen (5). The existence of these fibers makes it possible for the composite specimens to undergo substantial slips before failure. They act as ties preventing separation of the composite parts.

As the quantity of polymer in the PMC mix increases, so does the number of such "ties." This, in turn, gives rise to a higher binding force and consequently to a higher shear transfer strength. Thus, the observed increase is really due to increased polymer content. The same phenomenon increases PMC strength in the same manner as improved mortar aggregate bond increases concrete strength (12).

The increase in polymer fiber ties also means that for a given crack width or slip, a higher shear

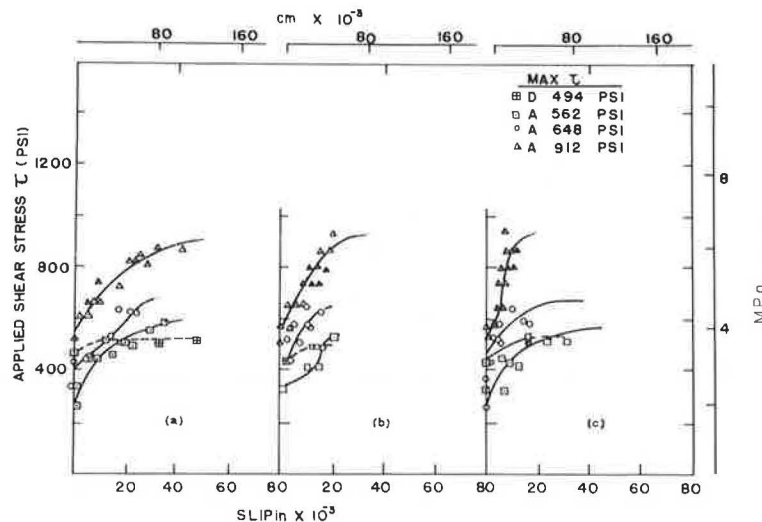


FIGURE 4 Applied shear stress  $\tau$  versus slip for series I specimens (no shear reinforcement) (a) avg slip measure =  $1/2 [\Delta 2-3 + \Delta 1-4]$ ; (b) dial gauge measure; and (c) microscope measure.

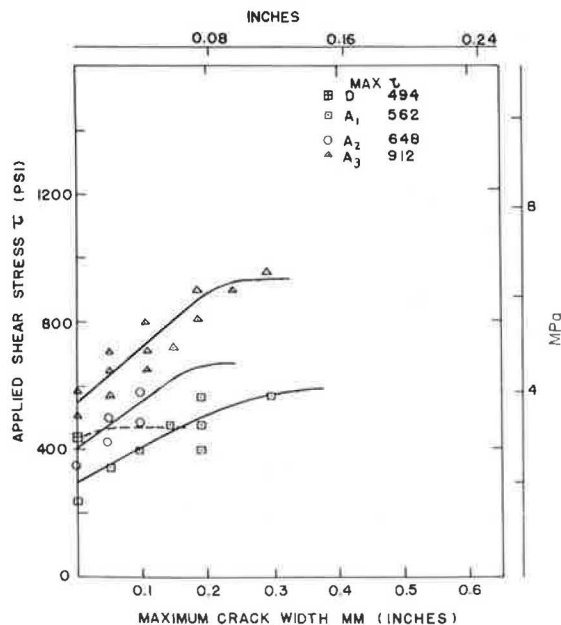


FIGURE 5 Applied shear stress  $\tau$  versus crack width for Series I specimens.

stress can be withstood by those specimens that have higher strength PMCs. Thus arises the increase in slope with PMC strength.

The observed ultimate slip of 0.5 mm (0.02 in.) indicates that the polymer fibers have a certain yield length. Beyond this length, no further increase in fiber load and, consequently, shear transfer resistance can be obtained.

The similarity between the ultimate capacities of the monolithically cast control specimens and the high-strength PMC composite ones shows that the bond between PMC and precast concrete in the composite specimens was so strong that failure occurred in the concrete part instead of at the shear plane.

#### Analysis of Series II Specimen Results

Unlike those of Series I, each of the specimens in this group exhibited a yield plateau, undergoing

slips of up to 2 mm (0.08 in.) before collapse. The specimens having shear transfer reinforcement had capacities increased with shear reinforcing strength (I). Figures 6 and 7 show that for a given maximum crack width and slip, an increase in I is accompanied by an increase in shear transfer resistance.

As the percentage of steel reinforcement is increased, the normal force exerted on the slip plane for a given crack width and slip increases. This results in higher shear transfer resistances for a given crack width or slip, as well as a higher shear transfer capacity with increasing I.

Visible cracks (by microscopy) appeared on these specimens between an applied stress of 429 to 643 psi. Failure in the heavily reinforced specimens was preceded by spalling of concrete near the exterior bars, suggesting the existence of high dowel forces.

#### Variation of Shear Transfer Capacity ( $v_t$ ) with Shear Reinforcing Strength (I)

The plots of  $v_t$  versus I in Figure 8 show a form similar to that postulated earlier. Between the range  $1.0 < I < 7.17$  MPa ( $150 < I < 1,040$  psi), the relationship between  $v_t$  and I is presumed linear. A least squares analysis of the data within this region gave the following results:

$$v_t = 0.609I + 711 \quad (17)$$

[The standard deviation in this expression is 336 Pa (48.8 psi).]

In Equation 17, 0.609 is the apparent coefficient of friction and 711 is the apparent cohesion (i.e., the maximum contribution to shear resistance due to bond).

It was observed that in specimens with  $I > 1,040$  psi, failure was induced by high dowel forces. So, shear transfer capacity was due primarily to dowel action of reinforcement. For high shear reinforcement  $I > 1,040$ , given by Equation 16. The plot in Figure 8 for this range gives the expression:

$$v_t = 0.20I + 1,140 \quad (18)$$

For  $I = 0$ , the 68.95 MPa (10,000 psi) PMC composite specimens gave a strength of 648 psi. This is



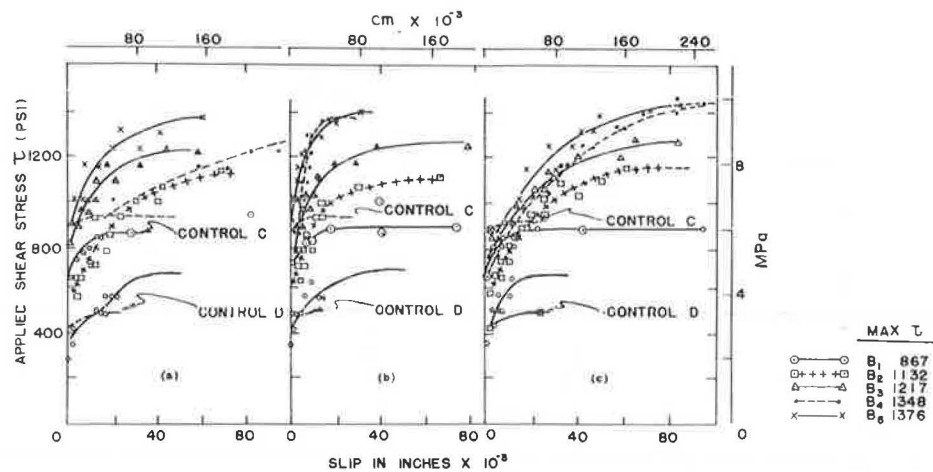


FIGURE 6 Applied shear stress  $\tau$  versus slip for Series II specimens (with shear reinforcement).

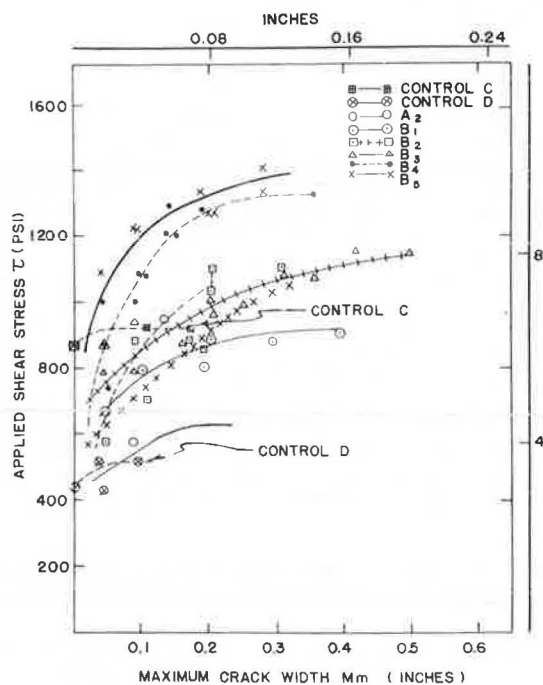


FIGURE 7 Applied shear stress  $\tau$  versus maximum crack width for Series II specimens.

TABLE 3 Comparison of ACI Shear Transfer Capacity Values with Those Given by Proposed Expressions

Shear Reinforcing Strength ( $I$ ) (psi)	Shear Transfer Capacity (psi)			Failure Experimental Results (5)
	Allowable by ACI Formula <sup>a</sup> $\mu = 1.0$ $\phi = 0.85$ (2)	By Hypothesis Equations 11, 13 (3)	Column 3 <sup>b</sup> 1.7 (4)	
0	0	648	381	647
100	85	648	381	-
286	243	885	520	867
572	486	1,059	622	1,132
858	729	1,233	725	1,217
1,073	(1,073) 800 <sup>a</sup>	1,355	797	1,348
1,375	(1,375) 800 <sup>a</sup>	1,415	832	1,376
1,500	(1,500) 800 <sup>a</sup>	1,440	847	-

Note: 1 psi = 6.895 Pa.

ACI Formula  $v_t = \phi \mu \bar{p} f_y$ , namely  $\phi \mu I$ .

<sup>a</sup>Limit of 800 psi for concrete by ACI code 318-83.

<sup>b</sup>Values based on a safety factor of 1.7.

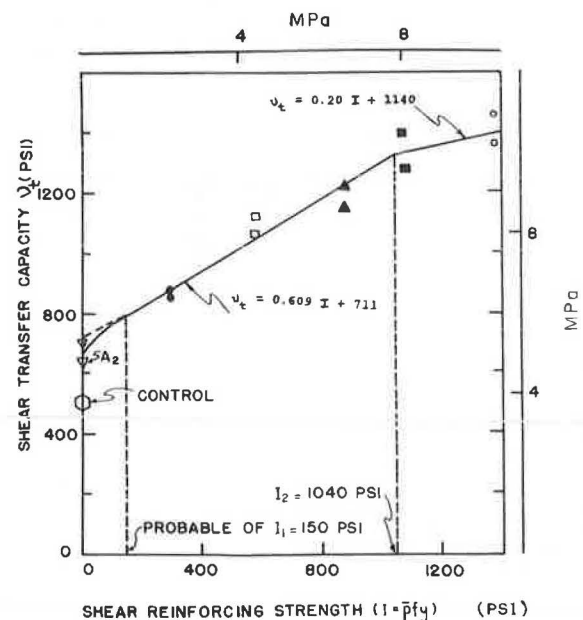


FIGURE 8 Shear transfer capacity  $v_t$  versus shear reinforcing strength  $I = \bar{p} f_y$  for L-prism specimens.

the resistance due to intrinsic bond. The range  $I = 0$  to  $I = 150$  psi is a transition stage where apparent cohesion increases with  $I$ .

The ACI code formula  $v_t = \phi \bar{p} f_y \mu < 800$  psi ( $\mu = 1.4 - 0.8$ ) basically ignores the apparent cohesion and presumably compensates for it by using high coefficient of friction values. When compared with experimental results (Table 3), it is observed that, initially, ACI values are unnecessarily conservative. But as  $I$  increases, the values obtained by the proposed shear transfer hypothesis as summarized in Equations 14 and 16 give allowable values comparable to the ACI limit of 800 psi, using a safety factor of 1.7 as in column 4 of Table 3.

#### CONCLUSIONS

The investigation has shown that the shear transfer capacity of concrete elements might be expressed as follows:

$$\begin{aligned} \text{For } I &= 0 & v_t &= C \\ I_1 &< I < I_2 & v_t &= I \mu' + C' \\ I &> I_2 & v_t &= GI + Q \end{aligned}$$

At any given value of  $I$ , the strength of the concrete under a condition of combined direct and shearing stresses gives the upper bound values for  $v_t$ .

The bond shear transfer capacity  $V_o$  appears to increase with concrete or PMC strength. It varies from 495 psi for concrete on concrete composite element with  $f_c = 5,000$  psi, to 920 psi for a PMC on concrete element of PMC strength = 12,000 psi (82.7 MPa).

For a composite element of 10,000 psi PMC on 5,000 psi precast concrete,  $C = 650$  psi;  $C' = 710$ ;  $\mu' = 0.609$ ;  $Q = 1,140$  psi;  $G = 0.20$ ;  $I_1 = 150$  psi; and  $I_2 = 1,040$  psi. On this basis,  $v_t = 0.609I + 711$  for  $150 < I < 1,040$  psi and  $v_t = 0.20I + 1,140$  for  $I > 1,040$ .

#### ACKNOWLEDGMENT

This paper is the result of the continuing polymer research at Rutgers University under the direction of the author and is based on the doctoral thesis of Maurice M. Ukadike.

#### NOTATIONS USED IN EQUATIONS

- $A_s'$  = Area of shear surface (in.<sup>2</sup>),  
 $A_s$  = Area of steel shear transfer reinforcement (in.<sup>2</sup>),  
 $C, C'$  = Apparent cohesion at  $\bar{\rho} = 0$  and  $\bar{\rho} > 0$ , respectively (psi)  
 $B$  = Bond force per unit area (psi)  
 $G = 1.564(f_c'/f_y)^{1/2}$  = A constant (dimensionless)  
 $I = \rho f_y$  = Shear reinforcing strength  
 $k_1$  = Ratio of bond area to total shear area  
 $k_2$  = Ratio of projected area of aggregates to total shear area  
 $k_3 = 1 - k_1 - k_2$   
 $P$  = Applied load (lb)  
 $Q = \rho f_y \mu$  = A constant for high values of  $\bar{\rho}$  (psi)  
 $\Delta V_b, \Delta V_d, \Delta V_f, \Delta V_i$  = Shear resisting loads due to bond, dowel action, friction, and aggregate interlock, respectively (lb)  
 $\Delta V_t$  = Total shear resisting load over the shear surface (lb)  
 $\bar{\rho} = A_s'/A$  = Ratio of steel shear reinforcement area to shear surface area  
 $\mu$  = Coefficient of friction  
 $\mu'$  = Apparent coefficient of friction  
 $v_b, v_d, v_f, v_i$  = Shear resistance due to bond, dowel action, friction, and aggregate interlock, respectively (psi)  
 $v_t$  = Total shear resistance (psi)  
 $\Delta i-j$  = Change in distance between points  $i$  and  $j$   
 $\tau$  = Applied shear stress (psi)  
 $f_y$  = Yield strength of dowel reinforcement (psi)

- $f_c'$  = Cylinder compressive strength  
 $b$  = Width of shear failure plane  
 $n'$  = Number of dowels  
 $T_f$  = Load transferred by dowel action per bar  
 $V_n$  = Sum of forces in the direction of plane  $n$   
 $w$  = Length of shear failure plane

#### REFERENCES

1. P.W. Birkeland and H.W. Birkeland. Connections in Precast Construction. Proc., American Concrete Institute, Vol. 63, No. 3, March 1966, pp. 345-367.
2. E.G. Nawy and M.M. Ukadike. Shear Transfer in Concrete and Polymer Modified Concrete Members Subjected to Shearing Loads. Journal of Testing and Evaluation, Vol. 11, No. 2, March 1983, pp. 89-99.
3. B. Bresler and K.S. Pister. Strength of Concrete Under Combined Stresses. Proc., American Concrete Institute, Vol. 55, Sept. 1958, pp. 321-345.
4. H. Dulacska. Dowel Action of Reinforcement Crossing Cracks in Concrete. Proc., American Concrete Institute, Vol. 69, No. 12, Dec. 1972, pp. 754-757.
5. R.D. Eash and H.H. Shafer. Reactions of Polymer Latex with Portland Cement. In Transportation Research Record 542, TRB, National Research Council, Washington, D.C., 1975, pp. 1-8.
6. R.C. Fenwick and T. Paulay. Mechanisms of Shear Resistance of Concrete Beams. Journal of the Structural Division, ASCE, Vol. 94, No. ST-10, Oct. 1968, pp. 2325-2350.
7. W. Han-Chin. Dual Failure Criterion for Plain Concrete. Proc., ASCE, Paper 10996, Vol. 100, EM6, Dec. 1974, pp. 1167-1181.
8. B.R. Hermansen and J. Cowan. Modified Shear Friction Theory for Bracket Design. Journal of the American Concrete Institute, Feb. 1974, pp. 55-57.
9. J.A. Hofbeck, I.A. Ibrahim, and A.H. Mattock. Shear Transfer in Reinforced Concrete. Proc., American Concrete Institute, Vol. 66, No. 2, Feb. 1969, pp. 119-128.
10. A.H. Mattock and N.M. Hawkins. Research on Shear Transfer in Reinforced Concrete. Journal of the Prestressed Concrete Institute, Vol. 17, No. 2, March-April 1972.
11. R.M. White and M.J. Holley. Experimental Studies of Membrane Shear Transfer. Journal of the Structural Division, ASCE, Vol. 98, No. ST-8, Aug. 1972, pp. 1835-1852.
12. P. Nepper-Christensen and P.H. Nielsen Tommy. Modal Determination of the Effect of Bond Between Coarse Aggregate and Mortar on the Compressive Strength of Concrete. Proc., American Concrete Institute, Vol. 66, No. 1, Jan. 1969, pp. 69-72.
13. M.M. Ukadike. Durability Strength and Shear Transfer Characteristics of Polymer Modified Concretes for Concrete Structural Systems. Ph.D. thesis. Rutgers University, New Brunswick, N.J., May 1978, pp. 132-150.
14. E.G. Nawy, M.M. Ukadike, and J. Sauer. High Strength Field Polymer Modified Concrete. Journal of the Structural Division, ASCE, Vol. 103, ST-12, 1977, pp. 2307-2322.